Received 24 June 2023, accepted 13 July 2023, date of publication 18 July 2023, date of current version 3 August 2023.

Digital Object Identifier 10.1109/ACCESS.2023.3296644

RESEARCH ARTICLE

Fractional Order Sliding Mode Control of Quadrotor Based on Fractional Order Model

ABDUL-WAHID A. SAIF[1,2], KHALED BIN GAUFAN[1,2], SAMI EL-FERIK[1,2], AND MUJAHED AL-DHAIFALLAH[1,3]

[1]Department of Control and Instrumentation Engineering, King Fahd University of Petroleum & Minerals (KFUPM), Dhahran 31261, Saudi Arabia
[2]Interdisciplinary Research Centre for Smart Mobility and Logistics (IRC-SML), KFUPM, Dhahran 31261, Saudi Arabia
[3]Interdisciplinary Research Centre for Renewable Energy and Power Systems (IRC-REPS), KFUPM, Dhahran 31261, Saudi Arabia

Corresponding author: Abdul-Wahid A. Saif (awsaif@kfupm.edu.sa)

This work was supported in part by the King Fahd University of Petroleum & Minerals (KFUPM) and in part by the Interdisciplinary Research Center for Smart Mobility and Logistics under Project INML2300.

ABSTRACT Quadrotor systems are becoming increasingly popular in various applications due to their maneuverability and versatility. Controlling these systems accurately is crucial to ensure stability and safety. This research paper proposes the implementation of two advanced controllers with integer and fractional order quadrotor systems. The purpose of the study is to enhance the control performance, robustness, and accuracy of the quadrotor system, and to highlight the potential of the proposed approach in modern control engineering. The researchers used simulation studies in MATLAB to verify the effectiveness of their approach. The results demonstrate that the implementation of Sliding Mode Control (SMC) and Fractional Order Sliding Mode Control (FOSMC) with the fractional order quadrotor system outperforms the traditional integer order quadrotor system in terms of control performance, robustness, and accuracy. Overall, the study highlights the potential of fractional order modeling and fractional order control techniques in improving the performance of quadrotor systems, which has significant implications for the advancement of modern control engineering.

INDEX TERMS Quadrotor model, sliding mode control, fractional order sliding mode control.

I. INTRODUCTION

Unmanned Vehicle Systems (UVS) are important for different areas nowadays because they can be controlled and operated remotely without human interference. UVS is a research key because of the increase in demand of remote sensing and control in wide range of applications such as scientific surveys, traffic surveillance, transportation aids, and inspection in addition to operation in harsh environments [22]. UVS have various configurations, characteristics, shapes and sizes which will be reflected on system dynamics [23]. The development in miniaturization of UVS offers high potential effort for small size and low cost of UVS compared to manned applications especially in certain applications. Rapid growing of UVS comes with promising future because of its size, cost, construction simplicity and maneuverability [13], [33].

The associate editor coordinating the review of this manuscript and approving it for publication was Xiwang Dong.

In order to design a controller for UVS, accurate models are needed to reflect system dynamics either by precise modelling or real time identification. UVS have a framework of rigid body dynamics and can be described by a set of differential equations using Euler-Lagrange.

In recent years, the exact model in many real systems has been shown to be more precise with fractional differential equations like viscoelastic systems [2], [28], electromagnetic theory [8], [15], economics [38], [39], and mechatronics [34]. In certain cases, dynamic fractional order equations are used to present several real systems. Over the last two decades, fractional system models were widely explored [1], [5], [14], [19], [26], [32], [35]. Thus, the conduct of too many existing systems, like viscoelastic systems, has been shown to be more reliable by fractional orders differential equations. In addition, Fractional systems were used widely in various scientific fields as successful approaches for modelling physical processes in the real world. In [3], non-integer systems for the explanation of long memory and inherited properties of complex phenomena have been investigated over the past years in various fields, including energy fuel [20], imaging science [42], biomedicine [19] and accident investigation [18]. A major example of fractional order systems is vibration systems that have many implementations in the industry and they are modelled by fractional order equations. According to [9], vibration systems with fractional order differential equations can be more accurately modelled and controlled. Up to date, numerous studies were carried out to explore the vibration system fractional order control [9].

The quadrotor is an unmanned aerial vehicle (UAV) that moves vertically to take off and land. Numerous research and studies have been conducted in recent years to model and regulate Quadrotors, see for example [45], [46], [47] and the references therein. Quadrotor UAVs are widely employed in a variety of applications due to their numerous advantages such as speed, smoothness, small size, and environmental friendliness [23].

Reference [7] introduced the use of PID and LQ control schemes on an indoor micro quadrotor, and it was discovered that these two types of controllers performed comparably and were capable of stabilizing the quadrotor's attitude around its hover position when subjected to minor disturbances [6].

Sliding mode control (SMC) consists of an algorithm that is fundamentally resilient in parameter, nonlinear, external, and insecure adjustments. It is introduced where the robustness criterion in driving systems is highly necessary in the face of strong uncertainty [22]. Backstepping is an iterative control approach that works on both linear and non-linear problems [21]. In a more recent paper, [25] and [43] proposed the use of backstepping and sliding-mode nonlinear control methods to control the quadrotor which gave a better performance in the presence of disturbances. Reference [11] proposed developing controllers that can stabilize the quadrotor in an outdoor environment, they compared the performance of an integral sliding-mode controller vs. a reinforcement learning controller and they reached a conclusion that both controllers were able to stabilize the quadrotor outdoors with improved performance over classical control technique.

In the field of rotor aircraft, different methods of typical control like PID and backstepping have been implemented [11], [16]. The attitude control systems were separated and defined as a first-order plus the lag time system and then the VTOL UAV fractional PI and [PI] flight controller design method [31]. The authors in [41] developed an autoregressive exogenous input (ARX) model to regulate VTOL UAV's pitch loop and converted them to FOPTD (first order plus time delay). In [41] proposed a sliding fractional order mode control method with an effective attitude controller which has a greater degree of freedom to achieve desired performance. Using Black–Nichols approach to control the quadrotor's position and attitude by implementing new approach of fraction order $PI^{\gamma}D^{\mu}$ [29]. In order to minimize the chattering and maximize the robustness of the dynamical response of UAV quad-rotor model, a fractional-order backstepping sliding mode control technique is implemented [36].

As represented in [29], sliding-mode controllers were used with fractional-order derivatives to theoretically mitigate chatter impacts. In [10], it was stated that a fractional order disruption observer could approximate the disorder, and a new fractional order sliding mode controller on the observer basis was recommended to minimize the chattering effect and monitoring errors. The authors in [40] proposed an adaptive SMC, including a slide surface with a fractional order integral part and a switching form with a less discord, means has less chattering. As shown in [4], to stabilize an uncertain non-linear fractional system, a sliding integral surface was formulated. In [44], two suggested approaches implemented integral fractional order sliding surface and various reaching laws to decrease the reach time and increase system performance. The SMC of fractional order nonlinear systems can be built using two methods, as shown in [17], [30], and [37]. The first relates to a class of fractional nonlinear systems, while the second applies to nonlinear systems of both fractional and integer order. The second strategy, which was outlined in [17], will be used in this research.

The primary objective of this work is to develop and see the improvements obtained in transforming the dynamics of a given nonlinear UAV system (transitional subsystem) into a fractional order one by implementing four controllers, SMC for integer and fractional UAV models, and FOSMC for integer and fractional UAV models.

The motivation for the research article that presents a novel approach to control both integer and fractional order quadrotor systems is to address the challenges associated with controlling these complex and non-linear systems. Quadrotor systems are widely used in various applications, such as aerial photography, search and rescue operations, and surveillance. However, they exhibit complex and non-linear dynamics, which pose significant challenges for control engineers.

The traditional integer-order control approaches may not be effective in controlling quadrotor systems due to the complex and non-linear dynamics. Fractional calculus provides a more accurate and comprehensive representation of quadrotor systems and their behavior. Therefore, the research article proposes a novel approach that utilizes two advanced controllers: Siding Mode Control (SMC) and Fractional Order Sliding Mode Control (FOSMC) to control both integer and fractional order quadrotor systems effectively.

The results of the study demonstrate the remarkable effectiveness of the proposed approach, as the implementation of SMC and FOSMC with the fractional order quadrotor system results in enhanced precision and robustness. The proposed approach has the potential to push the boundaries of modern control engineering and contribute to the development of more efficient and reliable control strategies for quadrotor systems.

This paper is organized as follows: Section II, briefly summarize the fractional calculus used in this paper. The modeling of the 6-DOF quadrotor system is presented in

Section III. Section IV subsequently goes through the problem statement. Section V presents the primary results: the SMC and FOSMC designs, as well as the stability analyses. Section VI depicts the simulation results and discussions, with Section VII delivering a conclusion and future work.

II. PRELIMINARIES

In this section, some insights to the fractional calculus which we will employ in our research are given. The adoption of the Gamma function is the first step in fractional calculus. The Gamma function, which is an extension of the principle of factorial numbers, is a significant special function in fractional mathematics. According to [47], the following is the function's general definition and what is indicated by the notation $\Gamma(y)$:

$$\Gamma(y)=\int_0^{\infty} e^{-t}t^{y-1}\,dt \tag{1}$$

The Caputo fractional derivative operator, employed in fractional-order dynamic equations, is defined using the Gamma function as follows [9]:

$$D_t^{\alpha}f(t)=\frac{1}{\Gamma(n-\alpha)}\int_0^{t}\frac{f^{(n)}(\tau)}{(t-\tau)^{\alpha-n+1}}d\tau,\quad 0<n\in Z \tag{2}$$

where $n-1<\alpha<n$.

It is worth noting that there are various definitions available for fractional order derivatives. Because the initial conditions for the fractional order differential equations with the Caputo derivatives are the same as for their counterparts in integer-order, the Caputo fractional derivative is more frequently utilized than other derivatives to describe the fractional order models. Thus, it is more typical to define the differential equations of fractional order using the Caputo fractional order.

III. MATHEMATICAL MODELLING OF UAV QUADROTOR

The quadrotor consists of four spinning propellers powered by four-dc engines that control vehicle motion. The quadrotor's position depends on the Euler angles, which are the angles of Roll (φ), Pitch (θ) and Yaw (ψ).

Rotors (1, 3) and rotors (2, 4) rotate in various ways to negate the moments produced by each other, as shown in FIGURE 1. The rolling velocity can be accomplished in the x-axis direction of the vehicle by increasing the angular momentum of the second rotor and decreasing its angular velocity by maintaining the entire rotation steady. Likewise, the pitch velocity along the y - axis is accomplished by increasing the third rotor angular velocity and reducing the first rotor angular velocity. And the motion of the yaw along the z-axis will increase the rotor velocity (1, 3) and reduce the rotor's velocity (2, 4). Also, the system consists of two frames (R^b *and* R^m) as shown in **FIGURE 1**

We will make the following assumptions:

- The quadrotor structure is rigid and symmetrical.
- The propellers are rigid.
- Thrust and drag are proportional to the square of the propellers speed

Under these assumptions, it is possible to describe the fuselage dynamics as that of a rigid body in space to which come to be added the aerodynamic forces caused by the rotation of the rotors. Using the formalism of Newton-Euler, the dynamic equations are written in the following form:

$$\begin{cases}\dot{\xi}=v\\ m\ddot{\xi}=f_f+f_t+f_g\\ \dot{R}=R\,S\,(\Omega)\\ J\dot{\Omega}=-\Omega\wedge J\Omega+\Gamma_f-\Gamma_a-\Gamma_g\end{cases} \tag{3}$$

See [25], to obtain more details of the derived dynamic equations (1). Table 1 explains the meaning of each parameter.

As a result, the following equations (4) and (5) are the whole dynamic model that governs the quadrotor, [12]:

$$\begin{cases}\ddot{\varphi}=a_1\dot{\psi}\dot{\theta}+b_1\Omega_r\dot{\theta}+c_1\dot{\varphi}^2+d_1U_2\\ \ddot{\theta}=a_2\dot{\psi}\dot{\varphi}+b_2\Omega_r\dot{\varphi}+c_2\dot{\theta}^2+d_2U_3\\ \ddot{\psi}=\mathrm{a}_3\dot{\varphi}\dot{\theta}+\mathrm{b}_3\dot{\psi}^2+\mathrm{c}_3\mathrm{U}_4\end{cases} \tag{4}$$

$$\begin{cases}\ddot{x}=a_4\dot{x}+b_4(c_\varphi s_\theta c_\psi+s_\varphi s_\psi)U_1\\ \ddot{y}=a_5\dot{y}+b_5(c_\varphi s_\theta s_\psi-s_\varphi c_\psi)U_1\\ \ddot{z}=a_6\dot{z}-g+b_6(c_\varphi c_\theta)U_1\end{cases} \tag{5}$$

where,

$$\begin{cases}a_1=\dfrac{I_{yy}-I_{zz}}{I_{xx}};\ b_1=-\dfrac{J_r}{I_{xx}};\ c_1=-\dfrac{K_{fx}}{I_{xx}};\\ d_1=\dfrac{l}{I_{xx}};\\ a_2=\dfrac{I_{zz}-I_{xx}}{I_{yy}};\ b_2=\dfrac{J_r}{I_{yy}};\ c_2=-\dfrac{K_{fy}}{I_{yy}};\\ d_2=\dfrac{l}{I_{yy}};\\ a_3=\dfrac{I_{xx}-I_{yy}}{I_{zz}};\ b_3=-\dfrac{K_{fz}}{I_{zz}};\ c_3=\dfrac{d}{I_{zz}}\\ a_4=-\dfrac{K_{tx}}{m};\ b_4=\dfrac{1}{m}\\ a_5=-\dfrac{K_{ty}}{m};\ b_5=\dfrac{1}{m}\\ a_6=-\dfrac{K_{tz}}{m};\ b_6=\dfrac{1}{m}\\ \Omega_r=\omega_1-\omega_2+\omega_3-\omega_4\end{cases} \tag{6}$$

The inputs for the quadrotor system are combinations of the rotors' speed (ω), which in this case is U_1 to control the altitude (z), and (U_2, U_3 and U_3) to control the angles (φ, θ and ψ), respectively. U_x and U_y are the virtual inputs that

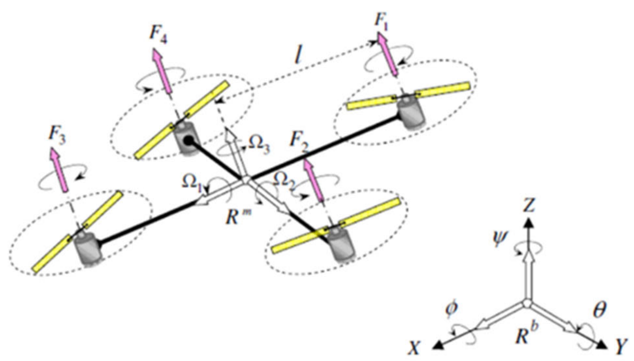

FIGURE 1. Quadrotor dynamic.

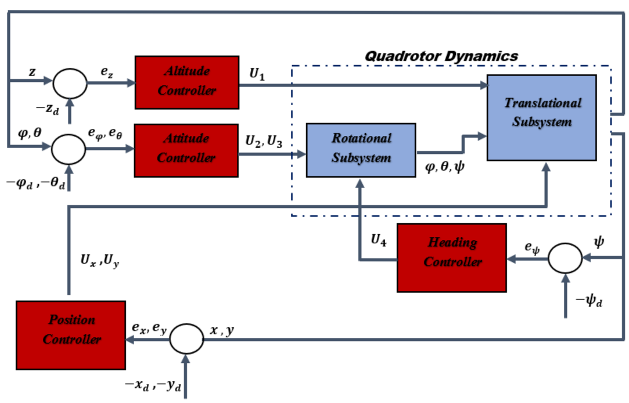

FIGURE 2. Quadrotor system controllers block diagram.

control quadrotor positions. All inputs are written as follows:

$$\begin{cases} \begin{pmatrix} U_1 \\ U_2 \\ U_3 \\ U_4 \end{pmatrix} = \begin{pmatrix} b & b & b & b \\ 0 & -b & 0 & b \\ -b & 0 & b & 0 \\ d & -d & d & -d \end{pmatrix} \begin{pmatrix} {\omega_1}^2 \\ {\omega_2}^2 \\ {\omega_3}^2 \\ {\omega_4}^2 \end{pmatrix} \\ U_x = c_\varphi s_\theta c_\psi + s_\varphi s_\psi \\ U_y = c_\varphi s_\theta s_\psi - s_\varphi c_\psi \end{cases} \tag{7}$$

where $c() \equiv \cos()$ *and* $s() \equiv \sin()$

FIGURE 2 shows the quadrotor block diagram with all system controllers. The controller blocks in the block diagram may include any type of control method, whether linear or nonlinear. All controller inputs are errors connected to some of the quadrotor states and provide an output that is either one or more control inputs U_1 through U_4 or φ_d *and* θ_d with U_x and U_y if it is the position controller.

IV. PROBLEM STATEMENT

A. INTEGER ORDER QUADROTOR SYSTEM

The quadrotor model in (4) and (5) can be recast in integer-order state space form as follows:

$$X = F(X) + G(X, U) \tag{8}$$

where $X = [x_1, \ldots, x_{12}]^T$ is the system state vector such as:

$$X = [\varphi, \dot{\varphi}, \theta, \dot{\theta}, \psi, \dot{\psi}, x, \dot{x}, y, \dot{y}, z, \dot{z}] \tag{9}$$

The following state representation is obtained from (8) and (9):

$$\begin{cases} \dot{x}_1 = x_2 \\ \dot{x}_2 = a_1 x_4 x_6 + b_1 \Omega_r x_4 + c_1 {x_2}^2 + d_1 U_2 \\ \dot{x}_3 = x_4 \\ \dot{x}_4 = a_2 x_2 x_6 + b_2 \Omega_r x_2 + c_2 {x_4}^2 + d_2 U_3 \\ \dot{x}_5 = x_6 \\ \dot{x}_6 = a_3 x_2 x_4 + b_3 {x_6}^2 + c_3 U_4 \\ \dot{x}_7 = x_8 \\ \dot{x}_8 = a_4 x_8 + b_4 U_x U_1 \\ \dot{x}_9 = x_{10} \\ \dot{x}_{10} = a_5 x_{10} + b_5 U_y U_1 \\ \dot{x}_{11} = x_{12} \\ \dot{x}_{12} = a_6 x_{12} - g + b_6 (c_\varphi c_\theta) U_1 \end{cases} \tag{10}$$

B. FRACTIONAL ORDER QUADROTOR SYSTEM

As an illustration of obtaining a fractional order system for integer one, assume the following dynamic system:

$$\mathrm{M}\ddot{\mathrm{Y}}(t) + \mathrm{C}\dot{\mathrm{Y}}(t) + \mathrm{KY}(t) = f \tag{11}$$

where $Y = [y_1, y_2, \ldots, y_n]^T \in R^n$ is the displacement vector and $M \in R^{n\times n}$ is the mass matrix and $C \in R^n$ is the

Damping matrix and the stiffness matrix is $K \in R^n$ and finally, $f \in R^r$ represents the input vector.

As shown in [9], this system can be transformed into a linear pseudo state space fractional order system as follows with fractional order, $\alpha = 0.5$:

Firstly, taking the state variables as:

$$\begin{cases} y_1(t) = y(t) \\ y_2(t) = D^{0.5} y(t) \\ y_3(t) = \dot{y}(t) \\ y_4(t) = D^{1.5} y(t) \end{cases} \tag{12}$$

Hence, (11) can be rewritten as follows using (12):

$$\begin{bmatrix} D^{0.5} y_1(t) \\ D^{0.5} y_2(t) \\ D^{0.5} y_3(t) \\ D^{0.5} y_4(t) \end{bmatrix} = \begin{bmatrix} 0 & I & 0 & 0 \\ 0 & 0 & I & 0 \\ 0 & 0 & 0 & I \\ -M^{-1}K & 0 & -M^{-1}C & 0 \end{bmatrix} \begin{bmatrix} y_1(t) \\ y_2(t) \\ y_3(t) \\ y_4(t) \end{bmatrix} + \begin{bmatrix} 0 \\ 0 \\ 0 \\ I \end{bmatrix} f \tag{13}$$

Then, the linear fractional order system form is:

$$D^{0.5} y(t) = AY(t) + Bf$$

where,

$$A = \begin{bmatrix} 0 & I & 0 & 0 \\ 0 & 0 & I & 0 \\ 0 & 0 & 0 & I \\ -M^{-1}K & 0 & -M^{-1}C & 0 \end{bmatrix} \text{ and } B = \begin{bmatrix} 0 \\ 0 \\ 0 \\ I \end{bmatrix}$$

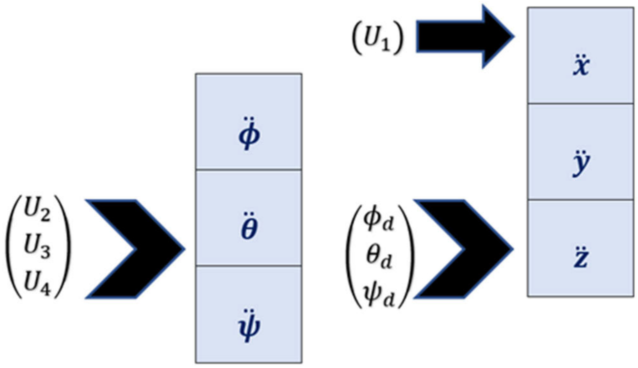

FIGURE 3. Rotational and transitional subsystems.

In this work, the transitional motion model of an UAV, equation (5), will be transformed into a fractional order one, while keeping the rotational equations (4) as integer. The following change of variables will be assumed:

$$\begin{cases} x_1 = x \\ x_2 = D^{0.5}x \\ x_3 = \dot{x} \\ x_4 = D^{1.5}x \end{cases} \tag{14}$$

$$\begin{cases} x_5 = y \\ x_6 = \mathrm{D}^{0.5}\mathrm{y} \\ x_7 = \dot{y} \\ x_8 = D^{1.5}y \end{cases} \tag{15}$$

$$\begin{cases} x_9 = \mathrm{z} \\ x_{10} = \mathrm{D}^{0.5}z \\ x_{11} = \dot{z} \\ x_{12} = D^{1.5}z \end{cases} \tag{16}$$

Hence, based on the above equations (14), (15), and (16) the translational equations of the quadrotor will be as follows:

$$\begin{cases} D^{0.5}x_1 = x_2 \\ D^{0.5}x_2 = x_3 \\ D^{0.5}x_3 = x_4 \\ D^{0.5}x_4 = a_4x_3 + b_4U_xU_1 \end{cases} \tag{17}$$

$$\begin{cases} D^{0.5}x_5 = x_6 \\ D^{0.5}x_6 = x_7 \\ D^{0.5}x_7 = x_8 \\ D^{0.5}x_8 = a_5x_7 + b_5U_yU_1 \end{cases} \tag{18}$$

$$\begin{cases} D^{0.5}x_9 = x_{10} \\ D^{0.5}x_{10} = x_{11} \\ D^{0.5}x_{11} = x_{12} \\ D^{0.5}x_{12} = a_6x_{11} - g + b_6(\,c_\varphi c_\theta)U_1 \end{cases} \tag{19}$$

Finally, the whole partial fractional order system of the quadrotor will be as follows:

$$\begin{cases} \dot{x_1} = x_2 \\ \dot{x_2} = a_1x_4x_6 + b_1\Omega_rx_4 + c_1{x_2}^2 + d_1U_2 \\ \dot{x_3} = x_4 \\ \dot{x_4} = a_2x_2x_6 + b_2\Omega_rx_2 + c_2{x_4}^2 + d_2U_3 \\ \dot{x_5} = x_6 \\ \dot{x_6} = a_3x_2x_4 + b_3{x_6}^2 + c_3U_4 \\ D^{0.5}x_{f\,7} = x_{f\,8} \\ D^{0.5}x_{f\,8} = x_{f\,9} \\ D^{0.5}x_{f\,9} = x_{f\,10} \\ D^{0.5}x_{f\,10} = a_4x_{f\,9} + b_4U_{x_f}U_{1f} \\ D^{0.5}x_{f\,11} = x_{f\,12} \\ D^{0.5}x_{f\,12} = x_{f\,13} \\ D^{0.5}x_{f\,13} = x_{f\,14} \\ D^{0.5}x_{f\,14} = a_5x_{f\,13} + b_5U_{y_f}U_{1f} \\ D^{0.5}x_{f\,15} = x_{f\,16} \\ D^{0.5}x_{f\,16} = x_{f\,17} \\ D^{0.5}x_{f\,17} = x_{f\,18} \\ D^{0.5}x_{f\,18} = a_6x_{f\,17} - g + b_6\left(c_\varphi c_\theta\right)U_{1_f} \end{cases} \tag{20}$$

V. CONTROL DESIGN

The quadrotor system is a 6 DOF because it has six outputs (φ, θ, ψ, x, y, z) but it has only four inputs that can be manipulated (U_1 , U_2 , U_3 , U_4); hence it is considered as a type of underactuated systems because the number of controlled variables (outputs) is more than the number of manipulated variables (inputs). Also, it can be observed that the rotational dynamics do not depend on the translational states; hence we can control the quadrotor attitude and heading (angular states ϕ , θ , ψ) separately by implementing three controllers (U_2 , U_3 , U_4) and form a rotational subsystem as an inner loop. While, the outer loop will govern the quadrotor system's position by delivering the altitude and position (translational states) with the controlled angles. Because the system is underactuated, the quadrotor position (x, y) cannot be driven directly. It can be controlled by manipulating the roll and pitch angles (φ , θ). As a result, the position is controlled by specifying desired roll and pitch angles (φ_d , θ_d) and applying them to their respective controllers as shown in **FIGURE 3**

Define U_x and U_y as,

$$\begin{cases} \mathrm{U_x} = \mathrm{c}_\varphi \mathrm{s}_\theta \mathrm{c}_\psi + \mathrm{s}_\varphi \mathrm{s}_\psi \\ U_y = c_\varphi s_\theta s_\psi - s_\varphi c_\psi \end{cases} \tag{21}$$

Solving (21) to obtain the desired angles φ_d and θ_d as follows:

$$\begin{cases} \varphi_d = \sin^{-1}[s_{\psi_d}U_x - c_{\psi_d}U_y] \\ \theta_d = \sin^{-1}[\frac{1}{c_{\varphi_d}}(c_{\psi_d}U_x + s_{\psi_d}U_y)] \end{cases} \tag{22}$$

TABLE 1. Quadrotor parameters description.

Parameters	Description	Units
ξ	Quadrotor Position with Respect to The Fame (R^b).	m
v	Quadrotor Velocity with Respect to The Fame (R^b).	m/s
m	Total Mass	kg
J	Inertia Matrix with Respect To R^m ($J \in R^{3x3}$)	$kg.m^2$
Ω	Angular Velocity Vector	m/rad
$S(\Omega)$	Skew-Symmetric Matrix	m/rad
f_f	Resultant of Four Rotors' Forces	N
f_t	Resultant of Drag Forces Along (X,Y,Z)	N
f_g	Gravity Force	m/s^2
Γ_f	Quadrotor Moment in R^b	$N.m$
Γ_a	Resultant of Aerodynamics Frictions Torques	$N.m$
Γ_g	Resultant of Torques Due to The Gyroscopic Effects	$N.m$
$[x,y,z]$	Integer Linear Position Vector	m
$[x_f,y_f,z_f]$	Fractional Order Linear Position Vector	m
$[\varphi,\theta,\psi]$	Angular Position Vector	rad
$[I_{xx},I_{yy},I_{zz}]$	Inertia Moment Vector	$kg.m^2$
$[K_{fx},K_{fy},K_{fz}]$	Rotational Drag Coefficients	$N/rad/s$
$[K_{tx},K_{ty},K_{tz}]$	Linear Drag Coefficients	$N/m/s$
J_r	Rotor Inertia Moment	$N.m/rad/s^2$

A. SLIDING MODE CONTROL DESIGN (SMD)

In this section, we will develop an SMC employing the technique stated in Efe [17] and it was chosen due to its significant advantages, which include guaranteeing Lyapunov stability (LF), robustness, and addressing all system nonlinearities.

1) SMC FOR INTEGER ORDER QUADROTOR SYSTEM

Define the sliding surfaces as in (23)and the Lyapunov functions as in (24).

$$S_i = \begin{cases} k_{i-1}\left(x_{i-1} - x_{(i-1)d}\right) + k_i\left(x_i - x_{id}\right), \\ i \in \{2,\ 4,\ 6,\ 8,\ 10,\ 12\} \end{cases} \tag{23}$$

where k is a positive constant vector ($k^T \in \mathbb{R}^n$), and x_d is the desired vector state to be tracked.

$$V_i = \left\{\frac{1}{2}S_i^2\right., i \in \{2,\ 4,\ 6,\ 8,\ 10,\ 12\} \tag{24}$$

From (23), we can define the sliding surfaces in terms of the states of the quadrotor as follow:

$$\begin{cases} S_\varphi = S_2 = k_1\left(x_1 - x_{1d}\right) + k_2\left(x_2 - x_{2d}\right) \\ S_\theta = S_4 = k_3\left(x_3 - x_{3d}\right) + k_4\left(x_4 - x_{4d}\right) \\ S_\psi = S_6 = k_5\left(x_5 - x_{5d}\right) + k_6\left(x_6 - x_{6d}\right) \\ S_x = S_8 = k_7\left(x_7 - x_{7d}\right) + k_8\left(x_8 - x_{8d}\right) \\ S_y = S_{10} = k_9\left(x_9 - x_{9d}\right) + k_{10}\left(x_{10} - x_{10d}\right) \\ S_z = S_{12} = k_{11}\left(x_{11} - x_{11d}\right) + k_{12}(x_{12} - x_{12d}) \end{cases} \tag{25}$$

To guarantee that the proposed sliding surfaces are stable, the requisite sliding condition ($S\dot{S} < 0$) must be satisfied. Using the proposed sliding surface, the control laws will be as follows:

$$\begin{cases} U_1 = \dfrac{1}{k_{12}b_6c_\varphi c_\theta}[-q_z sign\left(S_z\right) - k_z S_z \\ -k_{12}\left(a_6x_{12} - g - \dot{x}_{12d}\right) - k_{11}\left(x_{12} - \dot{x}_{11d}\right)] \\ U_2 = \dfrac{1}{k_2d_1}[-q_\varphi sgn\left(S_\varphi\right) - k_\varphi S_\varphi \\ -k_2\left(a_1x_4x_6 + b_1\Omega_r x_4 + c_1{x_2}^2 - \dot{x_{2d}}\right) \\ -k_1\left(x_2 - \dot{x}_{1d}\right)] \\ U_3 = \dfrac{1}{k_4d_2}[-q_\theta sign\left(S_\theta\right) - k_\theta S_\theta \\ -k_4\left(a_2x_2x_6 + b_2\Omega_r x_2 + c_2{x_4}^2 - \dot{x}_{4d}\right) \\ -k_3\left(x_4 - \dot{x}_{3d}\right)] \end{cases}$$

$$\begin{cases} U_4 = \dfrac{1}{k_6c_3}[-q_\psi sign\left(S_\psi\right) - k_\psi S_\psi \\ -k_6\left(a_3x_2x_4 + b_3{x_6}^2 - \dot{x}_{6d}\right) \\ -k_5\left(x_6 - \dot{x}_{5d}\right)] \\ U_x = \dfrac{1}{k_8b_4U_1}[-q_x sign\left(S_x\right) - k_x S_x \\ -k_8\left(a_4x_8 - \dot{x}_{8d}\right) - k_7\left(x_8 - \dot{x}_{7d}\right)] \\ U_y = \dfrac{1}{k_{10}b_5U_1}[-q_y sign\left(S_y\right) - k_y S_y \\ -k_{10}\left(a_5x_{10} - \dot{x}_{10d}\right) - k_9\left(x_{10} - \dot{x}_{9d}\right)] \end{cases} \tag{26}$$

where $(q_z,\ q_\varphi,\ q_\theta,\ q_\psi,\ q_x,\ q_y)$ and $(k_z,\ k_\varphi,\ k_\theta,\ k_\psi,\ k_x,\ k_y) > 0$

Proof of (26):

The altitude sliding mode controller (ASMC) is developed to track a reference trajectory z_d. From (10), the altitude dynamic is:

$$\begin{cases} \dot{x}_{11} = x_{12} \\ \dot{x}_{12} = a_6 x_{12} - g + b_6(c_\varphi c_\theta) U_1 \end{cases} \tag{27}$$

And the altitude sliding surface from (25)is:

$$S_z = S_{12} = k_{11}\,(x_{11} - x_{11d}) + k_{12}(x_{12} - x_{12d}) \tag{28}$$

Now, taking the 1^{st} derivative of (S_z) would result:

$$\dot{S}_z = -q_z sgn\,(S_z) - k_z S_z \tag{29}$$

where $-\,(q_z sgn\,(S_z) + k_z S_z)$ represents the discontinuous part that satisfies the reachability condition.

$$k_{11}\,(\dot{x_{11}} - \dot{x_{11d}}) + k_{12}\,(\dot{x_{12}} - \dot{x_{12d}}) = -q_z sgn\,(S_z) - k_z S_z \tag{30}$$

Substituting the altitude dynamic equations ($\dot{x_{11}}$ *and* $\dot{x_{12}}$) implies,

$$k_{11}\,(x_{12} - \dot{x_{11d}}) + k_{12}(a_6 x_{12} - g + b_6 c_\varphi c_\theta U_1 - \dot{x_{12d}}) = -q_z sgn\,(S_z) - k_z S_z \tag{31}$$

Therefore, from (31) the sliding control law of altitude, U_1 will be calculated as follows:

$$U_1 = \frac{1}{k_{12} b_6 c_\varphi c_\theta}\,[-q_z sign\,(S_z) - k_z S_z - k_{12}\,(a_6 x_{12} - g - \dot{x_{12d}}) - k_{11}\,(x_{12} - \dot{x_{11d}})] \tag{32}$$

To ensure stability, a Lyapunov function is applied as a positive definite function, and its rate must be negative definite or semi-negative definite.

From (24), the altitude Lyapunov function is defined as:

$$V_z = V_{12} = \frac{1}{2} S_z^2 \tag{33}$$

Taking the 1^{st} derivative as:

$$\begin{cases} \dot{V}_z = \dot{V}_{12} = S_z\,\dot{S}_z \\ \dot{V}_z = \dot{V}_{12} = S_z\,[k_{11}\,(x_{12} - \dot{x}_{11d}) \\ \quad + k_{12}\left(a_6 x_{12} - g + b_6 c_\varphi c_\theta U_1 - \dot{x}_{12d}\right)] \end{cases} \tag{34}$$

Now, substitute (U_1) and simplify the result,

$$\begin{cases} \dot{V}_z = \dot{V}_{12} = S_z\,\dot{S}_z \\ \dot{V}_z = \dot{V}_{12} = S_z\,[k_{11}\,(x_{12} - \dot{x}_{11d}) \\ \quad + (-q_z sign\,(S_z) - k_z S_z - k_{11}\,(x_{12} - \dot{x}_{11d}))] \\ \dot{V}_z = \dot{V}_{12} = S_z\,\,[-q_z sign\,(S_z) - k_z S_z] \\ \dot{V}_z = \dot{V}_{12} = -q_z\,|S_z| - k_z S_z^2 \leq 0 \end{cases} \tag{35}$$

which is negative $\forall\, t$, since $q_z\,,\ k_z\ > 0$

The same procedures are followed to compute U_2, U_3, U_4, U_x and U_y and test their stability by Lyapunov functions.

2) SMC FOR FRACTIONAL ORDER QUADROTOR SYSTEM

The sliding mode control (SMC) approach has been widely used for controlling nonlinear systems. In recent years, there

TABLE 2. Quadrotor parameters values, [12].

Parameter Symbol	Description	Value	Units
g	Acceleration due to gravity	9.81	m/s^2
m	Quadrotor Mass	0.486	Kg
L	Quadrotor Arm Length	0.225	m
I_{xx}	Inertia Moment around x	4.856 E-03	$\mathrm{Kg.\,m^2}$
I_{yy}	Inertia Moment around y	4.856 E-03	$\mathrm{Kg.\,m^2}$
I_{zz}	Inertia Moment around z	8.801 E-03	$\mathrm{Kg.\,m^2}$
K_{fx}	Rotational Drag Coefficient in x	5.5670 E-04	$N/rad/s$
K_{fy}	Rotational Drag Coefficient in y	5.5670 E-04	$N/rad/s$
K_{fz}	Rotational Drag Coefficient in z	6.3540 E-04	$N/rad/s$
K_{tx}	Linear Drag Coefficient in x	5.5670 E-04	$N/m/s$
K_{ty}	Linear Drag Coefficient in y	5.5670 E-04	$N/m/s$
K_{tz}	Linear Drag Coefficient in z	6.3540 E-04	$N/m/s$
J_r	Inertia Moment of Rotor	2.8385 E-05	$N.m\,/rad/s^2$
b	Lift Coefficient	2.923 E-05	$N.m\,/rad/s$
d	Drag Coefficient	1.12 E-06	$N.m\,/rad/s$

has been a growing interest in applying SMC to fractional order systems due to their potential advantages over integer order systems. The SMC of fractional order nonlinear systems can be built using two methods. The first method is based on a class of fractional nonlinear systems, which can be described by the Caputo fractional derivative. This method involves designing a sliding mode surface that can ensure the stability of the system. For example, consider a fractional order system described by the following equation:

$$D^\alpha x(t) = f\,(x(t)) \tag{36}$$

where D^α is the Caputo fractional derivative, α is the fractional order, $x(t)$ is the state variable, and $f(x(t))$ is the nonlinear function. By using the SMC approach, a sliding mode surface can be designed to ensure the stability of the system.

The second method applies to both fractional and integer order nonlinear systems. This method involves designing a sliding mode surface that can ensure the stability of the system. For example, consider a nonlinear system described by the following equation:

$$x(t) = f\,(x(t)) + g\,(x(t))\,u(t) \tag{37}$$

where $x(t)$ is the state variable, $f(x(t))$ is the nonlinear function, $g(x(t))$ is the control gain, $u(t)$ is the control input, and the dot represents the time derivative. By using the SMC

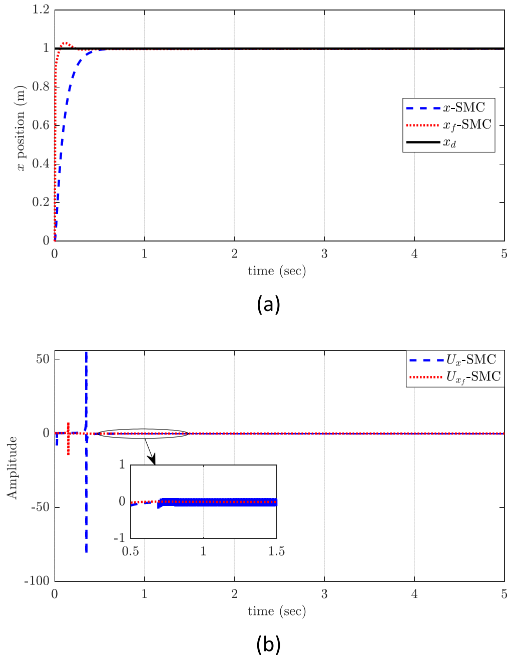

FIGURE 4. ***x*-Position under SMC (a) Time response (b) Control signal.**

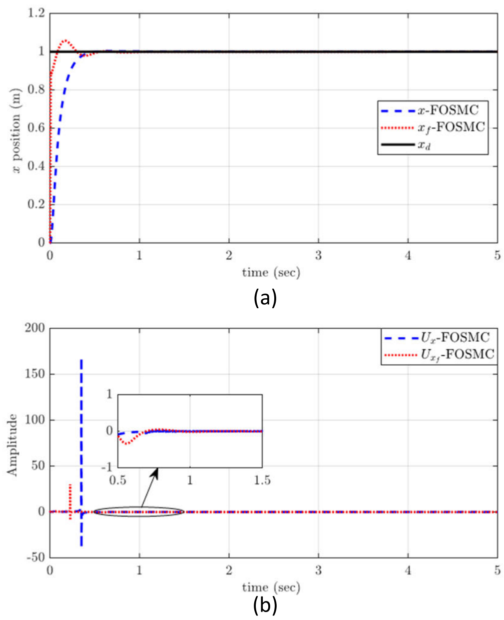

FIGURE 5. ***x*-Position under FOSMC (a) Time response (b) Control signal.**

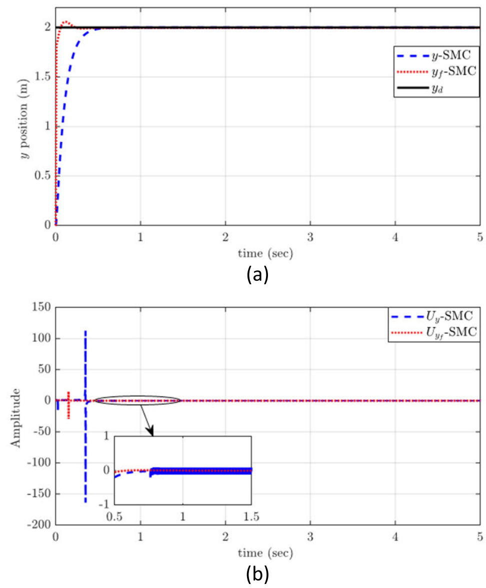

FIGURE 6. ***y*-Position under SMC (a) Time response (b) Control signal.**

approach, a sliding mode surface can be designed to ensure the stability of the system in the presence of disturbances. The control input $u(t)$ can be designed such that the system stays on the sliding mode surface.

Overall, the SMC approach can be an effective way to control fractional-order nonlinear systems. By using the two methods described above, a sliding mode surface can be designed to ensure the stability of the system, and the control input can be designed to keep the system on the sliding mode surface. Numerical examples of SMC applied to fractional order nonlinear systems have shown promising results in terms of stability and performance. For instance, the control of a fractional order chaotic system using SMC has been successfully demonstrated in [17]. Additionally, the control of a fractional order van der Pol oscillator using SMC has been investigated in [37], showing that the proposed method can effectively stabilize the system.

The proposed sliding mode controllers was applied to the fractional states (transitional equations), (20). Define the sliding surfaces and the Lyapunov functions as follow:

$$S_{f\,i} = \begin{cases} q_{i-3}\left(x_{f\,i-3} - x_{f\,(i-3)d}\right) \\ +q_{i-2}\left(x_{f\,i-2} - x_{f\,(i-2)d}\right) \\ +q_{i-1}\left(x_{f\,i-1} - x_{f\,(i-1)d}\right) \\ +q_i\left(x_{f\,i} - x_{f\,id}\right) \\ i \ \in \{10,\ 14,\ 18\} \end{cases} \tag{38}$$

where q is a positive constant vector ($q^T \in \mathbb{R}^n$), and $x_{f\,d} = x_d$ is the desired vector states to be tracked.

$$V_{f\,i} = \left\{\frac{1}{2}S_{f\,i}^2,\ i \ \in \{10,\ 14,\ 18\}\right. \tag{39}$$

From (38), we can define the sliding surfaces as follow:

$$\begin{cases} S_{f\,x} = S_{10} = q_7\left(x_{f\,7} - x_{f\,7d}\right) \\ +q_8\left(x_{f\,8} - x_{f\,8d}\right) + q_9\left(x_{f\,9} - x_{f\,9d}\right) \\ +q_{10}\left(x_{f\,10} - x_{f\,10d}\right) \\ S_{f\,y} = S_{14} = q_{11}\left(x_{f\,11} - x_{f\,11d}\right) \\ +q_{12}\left(x_{f\,12} - x_{f\,12d}\right) + q_{13}\left(x_{f\,13} - x_{f\,13d}\right) \\ +q_{14}\left(x_{f\,14} - x_{f\,14d}\right) \\ S_{f\,z} = S_{18} = q_{15}\left(x_{f\,15} - x_{f\,15d}\right) \\ +q_{16}\left(x_{f\,16} - x_{f\,16d}\right) + q_{17}\left(x_{f\,17} - x_{f\,17d}\right) \\ +q_{18}\left(x_{f\,18} - x_{f\,18d}\right) \end{cases} \tag{40}$$

To ensure the proposed sliding surfaces are stable, the necessary sliding condition ($S_f \dot{S}_f < 0$) must be verified. So, the control laws will be chosen as follows:

$$\begin{cases} U_{xf} = \dfrac{1}{q_{10} b_4 U_{1f}}[-\gamma_x sgn\left(S_{f\,x}\right) - \sigma_x S_{f\,x} \\ -q_7\left(x_{f\,8} - D^{0.5}x_{f\,7d}\right) \\ -q_8\left(x_{f\,9} - D^{0.5}x_{f\,8d}\right) \\ -q_9\left(x_{f\,10} - D^{0.5}x_{f\,9d}\right) \\ -q_{10}\left(a_4 x_{f\,9} - D^{0.5}x_{f\,10d}\right)] \\ U_{yf} = \dfrac{1}{q_{14} b_5 U_{1f}}[-\gamma_y sgn\left(S_{f\,y}\right) - \sigma_y S_{f\,y} \\ -q_{11}\left(x_{f\,12} - D^{0.5}x_{f\,11d}\right) \\ -q_{12}\left(x_{f\,13} - D^{0.5}x_{f\,12d}\right) \\ -q_{13}\left(x_{f\,14} - D^{0.5}x_{f\,13d}\right) \\ -q_{14}\left(a_5 x_{f\,13} - D^{0.5}x_{f\,14d}\right) \\ U_{1f} = \dfrac{1}{q_{18} b_6 c_\varphi c_\theta}[-\gamma_z sgn\left(S_{f\,z}\right) - \sigma_z S_{f\,z} \\ -q_{15}\left(x_{f\,16} - D^{0.5}x_{f\,15d}\right) \\ -q_{16}\left(x_{f\,17} - D^{0.5}x_{f\,16d}\right) \\ -q_{17}\left(x_{f\,18} - D^{0.5}x_{f\,17d}\right) \\ -q_{18}\left(a_6 x_{f\,17} - g - D^{0.5}x_{f\,18d}\right)] \end{cases} \tag{41}$$

where $(\gamma_x,\ \gamma_y,\ \gamma_z)$ and $(\sigma_x,\ \sigma_y,\ \sigma_z) > 0$, and constants.

Because the rotating subsystem was not subjected to the fractional scheme transformation, the sliding mode controllers for the fractional system are the same as for the integer system ($U_2,\ U_3$ *and* U_4), as given in (26).

Proof of (41):

From (20), the fractional order altitude dynamic (z_f) is:

$$\begin{cases} D^{0.5}x_{f\,15} = x_{f\,16} \\ D^{0.5}x_{f\,16} = x_{f\,17} \\ D^{0.5}x_{f\,17} = x_{f\,18} \\ D^{0.5}x_{f\,18} = a_6 x_{f\,17} - g + b_6(\ c_\varphi c_\theta)U_{1_f} \end{cases} \tag{42}$$

The altitude sliding surface for fractional system (42)is given in (40)as:

$$\begin{aligned} S_{f\,z} = S_{18} = q_{15}\left(x_{f\,15} - x_{f\,15d}\right) + q_{16}\left(x_{f\,16} - x_{f\,16d}\right) \\ + q_{17}\left(x_{f\,17} - x_{f\,17d}\right) + q_{18}\left(x_{f\,18} - x_{f\,18d}\right) \end{aligned} \tag{43}$$

Taking half derivative (for $\alpha = 0.5$) of both sides,

$$\begin{aligned} D^{0.5}S_{f\,z} = D^{0.5}S_{18} = q_{15}\left(D^{0.5}x_{f\,15} - D^{0.5}x_{f\,15d}\right) \\ + q_{16}\left(D^{0.5}x_{f\,16} - D^{0.5}x_{f\,16d}\right) \\ + q_{17}\left(D^{0.5}x_{f\,17} - D^{0.5}x_{f\,17d}\right) \\ + q_{18}\left(D^{0.5}x_{f\,18} - D^{0.5}x_{f\,18d}\right) \end{aligned} \tag{44}$$

Now, let

$$\begin{cases} D^{0.5}S_{f\,z} = -\gamma_z sgn\left(S_{f\,z}\right) - \sigma_z S_{f\,z} \\ q_{15}\left(D^{0.5}x_{f\,15} - D^{0.5}x_{f\,15d}\right) \\ +q_{16}\left(D^{0.5}x_{f\,16} - D^{0.5}x_{f\,16d}\right) \\ +q_{17}\left(D^{0.5}x_{f\,17} - D^{0.5}x_{f\,17d}\right) \\ +q_{18}\left(D^{0.5}x_{f\,18} - D^{0.5}x_{f\,18d}\right) \\ = -\gamma_z sgn\left(S_{f\,z}\right) - \sigma_z S_{f\,z} \\ \gamma_z \textit{ and } \sigma_z\ > 0 \end{cases} \tag{45}$$

Substituting ($D^{0.5}x_{f\,15}$, $D^{0.5}x_{f\,16}$, $D^{0.5}x_{f\,17}$, $D^{0.5}x_{f\,18}$) from the fractional dynamic altitude of the quadrotor given in (42)implies,

$$\begin{aligned} q_{15}\left(x_{f\,16} - D^{0.5}x_{f\,15d}\right) + q_{16}\left(x_{f\,17} - D^{0.5}x_{f\,16d}\right) \\ + q_{17}\left(x_{f\,18} - D^{0.5}x_{f\,17d}\right) \\ + q_{18}\left(a_6 x_{f\,17} - g + b_6 c_\varphi c_\theta U_{1_f} - D^{0.5}x_{f\,18d}\right) \\ = -\gamma_z sgn\left(S_{f\,z}\right) - \sigma_z S_{f\,z} \end{aligned} \tag{46}$$

Now, solving for U_{1f}:

$$\begin{aligned} U_{1f} = \frac{1}{q_{18} b_6 c_\varphi c_\theta}\Big[-\gamma_z sgn\left(S_{f\,z}\right) - \sigma_z S_{f\,z} \\ -q_{15}\left(x_{f\,16} - D^{0.5}x_{f\,15d}\right) \\ -q_{16}\left(x_{f\,17} - D^{0.5}x_{f\,16d}\right) - q_{17}\left(x_{f\,18} - D^{0.5}x_{f\,17d}\right) \\ -q_{18}\left(a_6 x_{f\,17} - g - D^{0.5}x_{f\,18d}\right)\Big] \end{aligned} \tag{47}$$

From (39), the Lyapunov function and its 1[st] derivative for the fractional system can be defined as:

$$\begin{cases} V_{f\,z} = V_{f\,18} = \dfrac{1}{2}S_{f\,z}^2 \\ \dot{V}_{f\,z} = \dot{V}_{f\,18} = \ S_{f\,z}\dot{S}_{f\,z} \end{cases} \tag{48}$$

We define $\mathfrak{D}^{0.5}S_{f\,z}$ as in (45):

$$\begin{cases} \mathfrak{D}^{0.5}S_{f\,z} = -\gamma_z sgn\left(S_{f\,z}\right) - \sigma_z S_{f\,z} \\ S_{f\,z} = -\gamma_z \mathfrak{D}^{-0.5} sgn\left(S_{f\,z}\right) - \sigma_z \mathfrak{D}^{-0.5}S_{f\,z} \\ \dot{S}_{f\,z} = -\gamma_z \mathfrak{D}^{0.5} sgn\left(S_{f\,z}\right) - \sigma_z \mathfrak{D}^{0.5}S_{f\,z} \\ ;\ \gamma_z \textit{ and } \sigma_z\ > \end{cases} \tag{49}$$

Now,

$$\begin{cases} \dot{V}_{f\,z} = \dot{V}_{f\,18} \\ = S_{f\,z}\left[-\gamma_z \mathfrak{D}^{0.5} sgn\left(S_{f\,z}\right) - \sigma_z \mathfrak{D}^{0.5}S_{f\,z}\right] \\ \dot{V}_{f\,z} = \dot{V}_{f\,18} = -\gamma_z \mathfrak{D}^{0.5}\left|S_{f\,z}\right| - \sigma_z D^{0.5}S_{f\,z}^2\ \leq 0 \end{cases} \tag{50}$$

$\mathfrak{D}^{0.5}\left|S_{f\,z}\right|$ and $D^{0.5}S_{f\,z}^2$ always positive as proved and discussed in [7] and [30], and this ensures that $S_{f\,z}\dot{S}_{f\,z} < 0$

The same steps are followed to compute U_{xf} and U_{yf} and test the stability by Lyapunov functions.

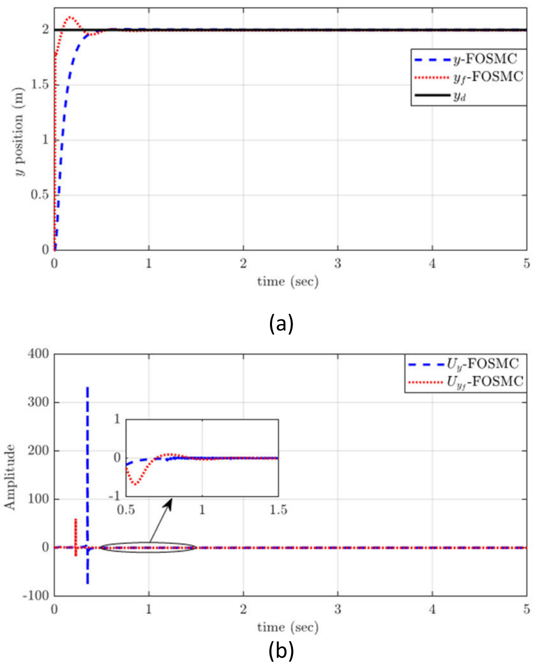

FIGURE 7. ***y*-Position under FOSMC (a) Time response (b) Control signal.**

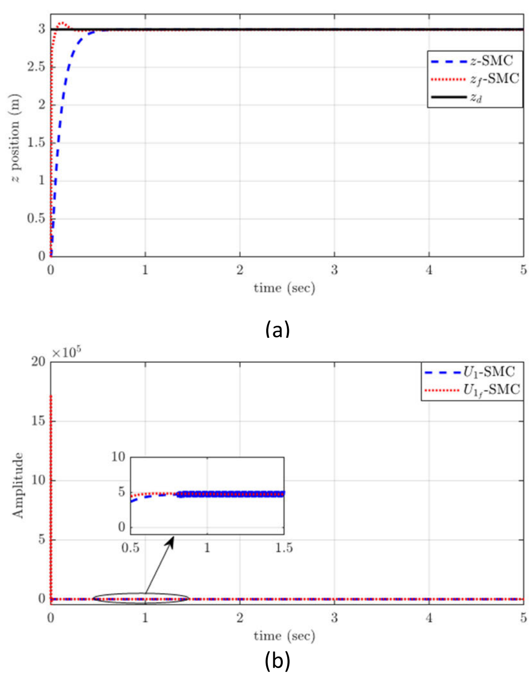

FIGURE 8. ***z*-Position under SMC (a) Time response (b) Control signal.**

B. FRACTIONAL ORDER SLIDING MODE CONTROL DESIGN (FOSMD)

Recently, the fractional order was added to the SMC to enhance the control system, and it is known as the FOSMC. In this section, we propose fractional order sliding mode controllers to control the integer quadrotor dynamic model's altitude, attitude, heading, and x, y positions.

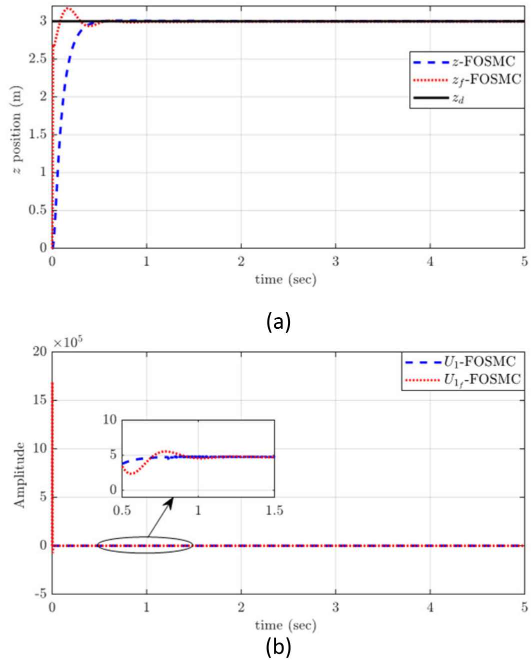

FIGURE 9. ***z*-Position under FOSMC (a) Time response (b) Control signal.**

1) FOSMC FOR INTEGER ORDER QUADROTOR SYSTEM

Define the fractional order sliding surfaces and the fractional order Lyapunov functions for the integer quadrotor system as follow:

$$\begin{cases} S_{FOSMC\,i} = k_{f\,i-1}\left(x_{i-1} - x_{(i-1)d}\right) \\ +k_{f_i}\mathrm{D}^{\gamma}\left(x_i - x_{id}\right) \\ V_{FOSMC\,i} = \dfrac{1}{2}S_{FOSMC\,i}^2 \\ i \in \{2,\ 4,\ 6,\ 8,\ 10,\ 12\} \end{cases} \tag{51}$$

Expanding (51), where $k_{f\,i}$ are constants, the fractional sliding surfaces are:

$$\begin{cases} S_{FOSMC\,\varphi} = S_{FOSMC_2} \\ = k_{f\,1}\left(x_1 - x_{1d}\right) + k_{f\,2}\mathrm{D}^{\gamma}\left(x_2 - x_{2d}\right), \\ S_{FOSMC\,\theta} = S_{FOSMC_4} \\ = k_{f\,3}\left(x_3 - x_{3d}\right) + k_{f\,4}\mathrm{D}^{\gamma}\left(x_4 - x_{4d}\right), \\ S_{FOSMC\,\psi} = S_{FOSMC_6} \\ = k_{f\,5}\left(x_5 - x_{5d}\right) + k_{f\,6}\mathrm{D}^{\gamma}\left(x_6 - x_{6d}\right), \\ S_{FOSMC\,x} = S_{FOSMC_8} \\ = k_{f\,7}\left(x_7 - x_{7d}\right) + k_{f\,8}\mathrm{D}^{\gamma}\left(x_8 - x_{8d}\right), \\ S_{FOSMC\,y} = S_{FOSMC_{10}} \\ = k_{f\,9}\left(x_9 - x_{9d}\right) + k_{f\,10}\mathrm{D}^{\gamma}\left(x_{10} - x_{10d}\right), \\ S_{FOSMC\,z} = S_{FOSMC_{12}} \\ = k_{f\,11}\left(x_{11} - x_{11d}\right) + k_{f\,12}\mathrm{D}^{\gamma}\left(x_{12} - x_{12d}\right) \end{cases} \tag{52}$$

Employing the same steps as in subsection VIto obtain the control laws of SMCs, we can derive the control laws of FOSMC and test the stability. The following results will be obtained:

$$\begin{cases} U_{FOSMC1} = \frac{1}{k_{12}b_6c_\varphi c_\theta}[-q_{z_f}D^{-\gamma}sgn\left(S_{FOSMCz}\right) \\ -k_{z_f}D^{-\gamma}S_{FOSMCz} - k_{12}\left(a_6x_{12} - g - \dot{x}_{12d}\right) \\ -k_{11}D^{-\gamma}\left(x_{12} - \dot{x}_{11d}\right)], \\ U_{FOSMC_2} = \frac{1}{d_1k_2}[-q_{\varphi_f}D^{-\gamma}sgn\left(S_{FOSMC\varphi}\right) \\ -k_{\varphi_f}D^{-\gamma}S_{FOSMC\varphi} \\ -k_2\left(a_1x_4x_6 + b_1\Omega_rx_4 + c_1x_2{}^2\right) + k_2x_{2d} \\ -k_1D^{-\gamma}\left(x_2 - \dot{x}_{1d}\right)], \\ U_{FOSMC3} = \frac{1}{d_2k_4}[-q_{\theta_f}D^{-\gamma}sgn\left(S_{FOSMC\theta}\right) \\ -k_{\theta_f}D^{-\gamma}S_{FOSMC\theta} \\ -k_4\left(a_2x_2x_6 + b_2\Omega_rx_2 + c_2x_4{}^2 - \dot{x}_{4d}\right) \\ -k_3D^{-\gamma}\left(x_4 - \dot{x}_{3d}\right)], \\ U_{FOSMC_4} = \frac{1}{c_3k_6}[-q_{\psi_f}D^{-\gamma}sgn\left(S_{FOSMC\psi}\right) \\ -k_{\psi_f}D^{-\gamma}S_{FOSMC\psi} \\ -k_6\left(a_3x_2x_4 + b_3x_6{}^2 - \dot{x}_{6d}\right) \\ -k_5D^{-\gamma}\left(x_6 - \dot{x}_{5d}\right)], \\ U_{FOSMCx} = \frac{1}{k_8b_4U_1}[-q_{x_f}\mathrm{D}^{-\gamma}sign\left(S_{FOSMCx}\right) \\ -k_{x_f}\mathrm{D}^{-\gamma}S_{FOSMCx} \\ -k_8\left(a_4x_8 - \dot{x}_{8d}\right) - k_7\mathrm{D}^{-\gamma}\left(x_8 - \dot{x}_{7d}\right)], \\ U_{FOSMCy} = \frac{1}{k_{10}b_5U_1}[-q_{y_f}\mathrm{D}^{-\gamma}sign\left(S_{FOSMCy}\right) \\ -k_{y_f}\mathrm{D}^{-\gamma}S_{FOSMCy} \\ -k_{10}\left(a_5x_{10} - \dot{x}_{10d}\right) - \mathrm{D}^{-\gamma}k_9\left(x_{10} - \dot{x}_{9d}\right)] \end{cases} \tag{53}$$

$$\begin{cases} V_{FOSMC_{12}} = \frac{1}{2}S^2_{FOSMC_{12}} \\ \dot{V}_{FOSMC_z} = \dot{V}_{FOSMC_{12}} = S_{FOSMC_{12}}\,\dot{S}_{FOSMC_{12}} \\ = \;-q_{z_f}\left|S_{FOSMC_z}\right| - k_{z_f}S^2_{FOSMC_z} \\ S_{FOSMC_z}\left[k_{11}\left(x_{12} - \dot{x}_{11d}\right)\right. \\ \left.+k_{12}\left(a_6x_{12} - g + b_6c_\varphi c_\theta U_1 - \dot{x}_{12d}\right)\right] \\ = -q_{z_f}\left|S_{FOSMC_z}\right| - k_{z_f}S^2_{FOSMC_z} \le 0 \end{cases} \tag{54}$$

which is negative $\forall\, t$, since $q_{zf}\,,\ k_{zf}\ > 0$

2) FOSMC FOR FRACTIONAL ORDER QUADROTOR SYSTEM

Define the fractional order sliding surfaces and the fractional order Lyapunov functions for the fractional order quadrotor system as follow:

$$\begin{cases} S_{FOSMCf\,i} = \begin{cases} q_{i-3}\left(x_{f\,i-3} - x_{f\,(i-3)d}\right) \\ +q_{i-2}\left(x_{f\,i-2} - x_{f\,(i-2)d}\right) \\ +q_{i-1}\left(x_{f\,i-1} - x_{f\,(i-1)d}\right) \\ +q_iD^\gamma\left(x_{f\,i} - x_{f\,id}\right) \end{cases} \\ V_{FOSMCf\,i} = \left\{\frac{1}{2}S^2_{FOSMC\,i}\right., \end{cases}$$

$$\backslash\, i\ \in \{\,10,\ 14,\ 18\} \tag{55}$$

From (55)), we can define the fractional sliding surfaces for fractional system as fractional order dynamic equations as follows:

$$\begin{cases} S_{FOSMCf\,10} = \\ q_7\left(x_{f\,7} - x_{f\,7d}\right) + q_8\left(x_{f\,8} - x_{f\,8d}\right) \\ +q_9\left(x_{f\,9} - x_{f\,9d}\right)q_{10}\boldsymbol{D^\gamma}\left(x_{f\,10} - x_{f\,10d}\right) \\ S_{FOSMCf\,14} = \\ q_{11}\left(x_{f\,11} - x_{f\,11d}\right) + q_{12}\left(x_{f\,12} - x_{f\,12d}\right) \\ +q_{13}\left(x_{f\,13} - x_{f\,13d}\right) + q_{14}\boldsymbol{D^\gamma}\left(x_{f\,14} - x_{f\,14d}\right) \\ S_{FOSMCf\,18} = \\ q_{15}\left(x_{f\,15} - x_{f\,15d}\right) + q_{16}\left(x_{f\,16} - x_{f\,16d}\right) \\ +q_{18}\boldsymbol{D^\gamma}\left(x_{f\,18} - x_{f\,18d}\right) + q_{17}\left(x_{f\,17} - x_{f\,17d}\right) \end{cases} \tag{56}$$

And the fractional order sliding mode control laws can be obtained using the same procedure as in subsection VII. The results are as follow:

$$\begin{cases} U_{FOSMCf\,1} = \frac{1}{b_6q_{18}c_\varphi c_\theta}[\\ -\rho_zD^{-\gamma}sgn\left(S_{FOSMCf\,18}\right) - \kappa_zD^{-\gamma}S_{FOSMCf\,18} \\ -q_{15}D^{-\gamma}\left(x_{f\,16} - D^{0.5}x_{f\,15d}\right) \\ -q_{16}D^{-\gamma}\left(x_{f\,17} - D^{0.5}x_{f\,16d}\right) \\ -q_{17}D^{-\gamma}\left(x_{f\,18} - D^{0.5}x_{f\,17d}\right) \\ -q_{18}\left(a_6x_{f\,17} - g - D^{0.5}x_{f\,18d}\right) \\ ] \\ \\ U_{FOSMCf\,x} = \frac{1}{q_{10}\mathrm{b}_4U_1}[\\ -\rho_xsgnD^{-\gamma}\left(S_{FOSMCf\,10}\right) - \kappa_xD^{-\gamma}S_{FOSMCf\,10} \\ -q_7D^{-\gamma}\left(x_{f\,8} - D^{0.5}x_{f\,7d}\right) \\ -q_8D^{-\gamma}\left(x_{f\,9} - D^{0.5}x_{f\,8d}\right) \\ -q_9D^{-\gamma}\left(x_{f\,10} - D^{0.5}x_{f\,9d}\right) \\ -q_{10}\left(a_4x_{f\,9} - D^{0.5}x_{f\,10d}\right) \end{cases}$$

$$\begin{cases} U_{FOSMCf\,y} = \frac{1}{q_{14}b_5U_1}[\\ -\rho_xD^{-\gamma}sgn\left(S_{FOSMCf\,14}\right) - \kappa_xD^{-\gamma}S_{FOSMCf\,14} \\ -q_{11}D^{-\gamma}\left(x_{f\,12} - D^{0.5}x_{f\,11d}\right) \\ -q_{12}D^{-\gamma}\left(x_{f\,13} - D^{0.5}x_{f\,12d}\right) \\ -q_{13}D^{-\gamma}\left(x_{f\,14} - D^{0.5}x_{f\,13d}\right) \\ -q_{14}D^{-\gamma}\left(a_5x_{f\,13} - D^{0.5}x_{f\,14d}\right) \\ ] \end{cases} \tag{57}$$

Following the same procedure in part 7and after simplifications, the LFs that ensure the stability of the proposed

TABLE 3. Case studies input signals.

	Case (1)	Case (2)
States	Reference Trajectory	Reference Trajectory
$\boldsymbol{x}$	$u(t)$	$cos(t)$
$\boldsymbol{y}$	$2u(t)$	$sin(t)$
$\boldsymbol{z}$	$3u(t)$	$0.2t$
$\boldsymbol{\psi}$	$5u(t)$	$u(t)$

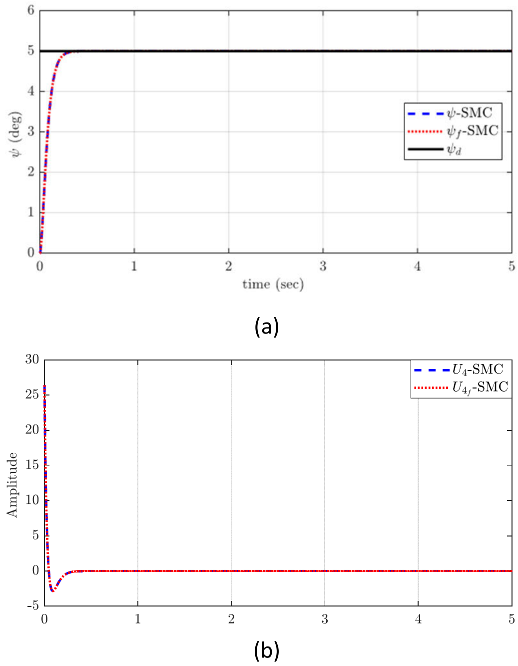

FIGURE 10. ψ-Angle under SMC (a) Time response (b) Control signal.

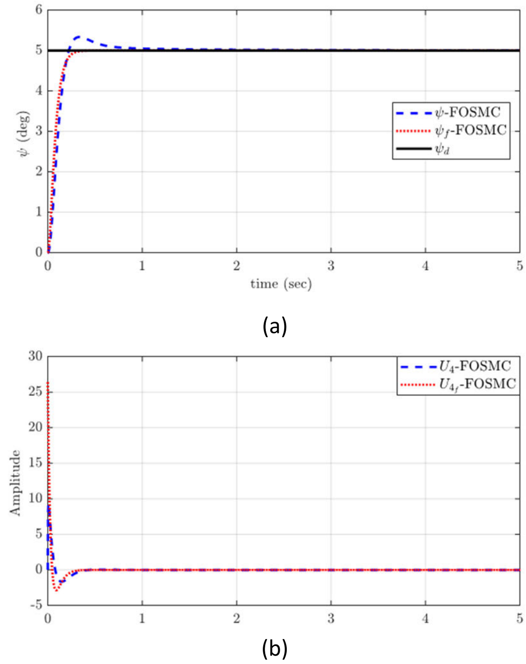

FIGURE 11. ψ-Angle under FOSMC (a) Time response (b) Control signal.

fractional sliding surfaces are as follow:

$$\begin{cases} \dot{V}_{FOSMC_{14}} = & -\rho_x D^{0.5}|S_{FOSMC_{14}}| - \kappa_x S^2_{FOSMC_{10}} \\ \dot{V}_{FOSMC_{14}} = & -\rho_y D^{0.5}|S_{FOSMC_{14}}| - \kappa_y S^2_{FOSMC_{14}} \\ \dot{V}_{FOSMC_{18}} = & -\rho_z D^{0.5}|S^2_{FOSMC_{18}}| - \kappa_z S^2_{FOSMC\,18} \end{cases} \tag{58}$$

$D^{0.5}\,|S_{FOSMC\,i}|$ *and* $S^2_{FOSMC\,i}$ always positive and as shown in Efe [17]; Khan et al. [30], and this ensures that $S_{FOSMC\,i}\dot{S}_{FOSMC\,i} < 0$ for all $i \in \{10, 14, 18\}$, and positive constants (ρ_x, ρ_y, ρ_z) and $(\kappa_x, \kappa_y, \kappa_z)$.

VI. SIMULATION RESULTS

MATLAB/Simulink has been used to test and simulate both integer and fractional order quadrotor systems by applying the proposed SMC and FOSMC. The PC utilized in the simulation is an HP model, featuring a Core(TM) i7-4702MQ CPU operating at a clock speed of 2.20GHz, accompanied by 8 GB of RAM. Additionally, we utilized MATLAB version 2022a throughout our investigation. For the fractional calculus, FOMCON Toolbox was utilized. **TABLE 1** shows the values of the quadrotor parameters employed in the simulations. Two case studies that have been investigated to highlight the issues that the quadcopter control systems in both integer and fractional systems may face in achieving the required tracking. The first case study was the step input, and the second one was the helical path. The states with reference trajectories of these case studies are presented **TABLE 2**.

Case Study (1) The positions (x, y and z) and the yaw (ψ) have been set as unit step references (x_d, y_d, z_d and ψ_d). The curves in **FIGURE 4, FIGURE 5, FIGURE 6, FIGURE 7, FIGURE 8** and **FIGURE 9**(a) show the responses of both integer and fractional position states under both controllers (SMC and FOSMC), while (b) represent the control input signals produced by the proposed controllers to acquire the desired positions. The output responses of yaw orientation in both integer and fractional systems are shown in **FIGURE 10** and **FIGURE 11**. As can be observed, the output responses in the fractional quadrotor system under both controllers (SMC and FOSMC) are speedier than that in the integer system. Furthermore, once SMC is used in integer systems, chattering occurs, that is alleviated via using FOSMC, although this phenomenon does not exist in fractional systems. **TABLE 4** and **TABLE 5** show the summary of the systems (integer/fractional ones) performance in terms of percentage overshoot OS, and rising time RT under SMC and FOSMC respectively, and it can be seen that the rising time in the fractional system is much faster than in the integer system;

TABLE 4. Time domain specifications of both systems under SMC.

	Integer System		Fractional System	
	$T_r(sec)$	$M_p(\%)$	$T_r(sec)$	$M_p(\%)$
x	0.216	0.505	0.008	0.874
y	0.217	0.505	0.008	0.890
z	0.217	0.505	0.0079	0.895
ψ	0.139	0.504	0.139	0.504

TABLE 5. Time domain specifications of both systems under FOSMC.

	Integer System		Fractional System	
	$T_r(sec)$	$M_p(\%)$	$T_r(sec)$	$M_p(\%)$
x	0.200	0.505	0.023	5.31
y	0.200	0.505	0.023	5.28
z	0.200	0.505	0.023	5.24
ψ	0.143	6.99	0.139	0.504

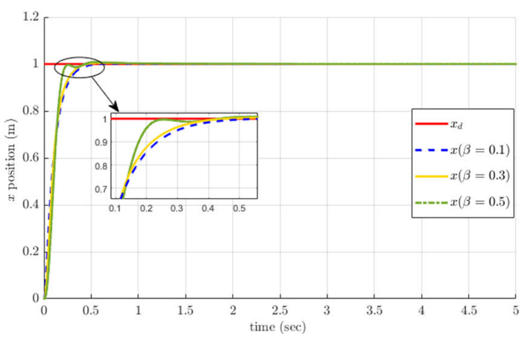

FIGURE 12. x-Position with different fractional orders, β.

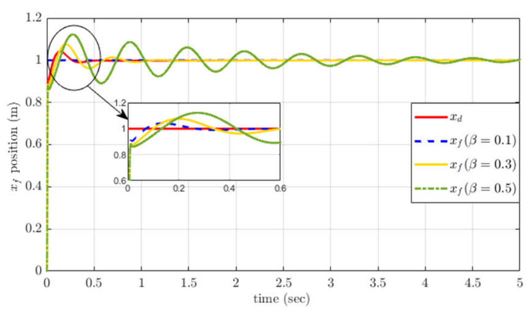

FIGURE 13. x_f-Position with different fractional orders, β.

nevertheless, the overshoot in the fractional system does not improve, but it is still acceptable in practice.

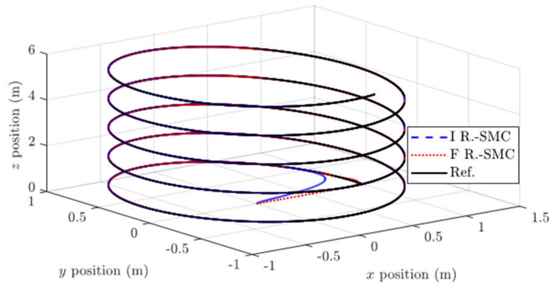

FIGURE 14. Case 2 - Helical trajectory under SMC.

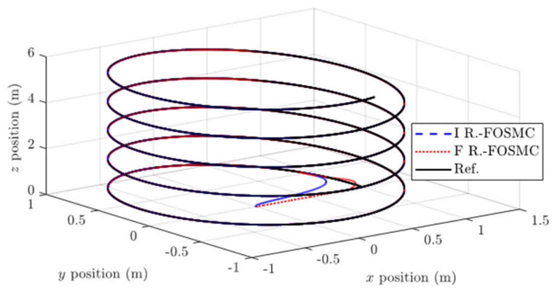

FIGURE 15. Case 2 - Helical trajectory under FOSMC.

Case Study (2) the second case study was the helical path. The states with reference trajectories are presented in **TABLE 3**.

FIGURE 12 and **FIGURE 13** show the x and x_f position with different fractional orders. The fractional order has significantly reduced the chattering of the controller. However, this increase in the fractional order affects the transient performance of the outputs of the quadrotor. Furthermore, the results reveal that decreasing the value of fractional order in FOSMC performs well in the fractional system but poorly in the integer system, however increasing that value of fractional order yields the opposite results. The fractional order parameters (β) were chosen to produce high output performance as well as better control input behaviour. They were not chosen to reduce the chattering at the expense of system performance, and vice versa. Hence, there is a trade-off between both behaviours.

FIGURE 14 and **FIGURE 15** show the tracking of integer and fractional quadrotor systems under both SMC and FOSMC respectively. The stated controllers followed the desired trajectory with less time in fractional system than in integer system and they almost have the same tracking error ($e_{track} \cong 0$).

VII. CONCLUSION AND FUTURE WORK

The study concludes that fractional order sliding mode control (FOSMC) is a viable method for controlling quadrotor systems and following a desired trajectory. FOSMC provides improved accuracy and robustness compared to traditional sliding mode control (SMC). The fractional derivative approach in FOSMC enables the system to have better tracking capabilities, which leads to reduced overshoot and rising time compared to SMC. Additionally, FOSMC also has a faster response rate compared to SMC, making it a better option for applications where fast control response is required. Overall, the study finds that FOSMC is a promising control method for controlling quadrotors and following a desired trajectory. In the near future work, we will investigate the performance of the proposed model by employing an aggressive disturbance rejection control paradigm to actively reject wind disturbances and reduce the influence of measurement noise.

REFERENCES

[1] H.-S. Ahn, Y. Chen, and I. Podlubny, "Robust stability test of a class of linear time-invariant interval fractional-order system using Lyapunov inequality," *Appl. Math. Comput.*, vol. 187, no. 1, pp. 27–34, Apr. 2007, doi: 10.1016/j.amc.2006.08.099.

[2] A. A. Jarbouh, "Rheological behaviour modelling of viscoelastic materials by using fractional model," *Energy Proc.*, vol. 19, pp. 143–157, Jan. 2012, doi: 10.1016/j.egypro.2012.05.194.

[3] E. S. A. Shahri, A. Alfi, and J. A. T. Machado, "Stability analysis of a class of nonlinear fractional-order systems under control input saturation," *Int. J. Robust Nonlinear Control*, vol. 28, no. 7, pp. 2887–2905, May 2018, doi: 10.1002/rnc.4055.

[4] R. Ayad, W. Nouibat, M. Zareb, and Y. B. Sebanne, "Full control of quadrotor aerial robot using fractional-order FOPID," *Iranian J. Sci. Technol., Trans. Electr. Eng.*, vol. 43, pp. 349–360, Jul. 2019, doi: 10.1007/s40998-018-0155-4.

[5] A. T. Azar and F. E. Serrano, "Robust control for asynchronous switched nonlinear systems with time varying delays," in *Proc. Int. Conf. Adv. Intell. Syst. Inform.*, vol. 533, 2017, pp. 891–899, doi: 10.1007/978-3-319-48308-5_85.

[6] A. Azzam and X. Wang, "Quad rotor arial robot dynamic modeling and configuration stabilization," in *Proc. 2nd Int. Asia Conf. Inform. Control, Automat. Robot.*, 2010, pp. 438–444. [Online]. Available: https://ieeexplore.ieee.org/abstract/document/5456804/

[7] M. Bailey. (2012). *Unmanned Aerial Vehicle Path Planning and Image Processing for Orthoimagery and Digital Surface Model Generation*. [Online]. Available: https://core.ac.uk/download/pdf/216051590.pdf

[8] D. Baleanu, A. K. Golmankhaneh, and A. K. Golmankhaneh, "On electromagnetic field in fractional space," *Nonlinear Anal., Real World Appl.*, vol. 11, no. 1, pp. 288–292, Feb. 2010, doi: 10.1016/j.nonrwa.2008.10.058.

[9] S. Balochian and N. Rajaee, "Fractional-order optimal control of fractional-order linear vibration systems with time delay," *Int. J. Syst. Dyn. Appl.*, vol. 7, no. 3, pp. 72–93, Jul. 2018, doi: 10.4018/ijsda.2018070104.

[10] S. Bouabdallah and S. Roland, "Backstepping and sliding-mode techniques applied to an indoor micro quadrotor," in *Proc. IEEE Int. Conf. Robot. Automat.*, Apr. 2005, pp. 2247–2252. [Online]. Available: https://ieeexplore.ieee.org/abstract/document/1570447/

[11] S. Bouabdallah, A. Noth, and R. Siegwart, "PID vs LQ control techniques applied to an indoor micro quadrotor," in *Proc. IEEE/RSJ Int. Conf. Intell. Robots Syst. (IROS)*, Sep. 2004, pp. 2451–2456, doi: 10.1109/IROS.2004.1389776.

[12] H. Bouadi, M. Bouchoucha, and M. Tadjine, "Sliding mode control based on backstepping approach for an UAV type-quadrotor," *World Academy Sci., Eng. Technol.*, vol. 26, no. 5, pp. 22–27, 2007.

[13] D. Chabot, "Trends in drone research and applications as the *Journal of Unmanned Vehicle Systems* turns five," *J. Unmanned Vehicle Syst.*, vol. 6, no. 1, Mar. 2018, doi: 10.1139/juvs-2018-0005.

[14] Y. Chen, H.-S. Ahn, and I. Podlubny, "Robust stability check of fractional order linear time invariant systems with interval uncertainties," *Signal Process.*, vol. 86, no. 10, pp. 2611–2618, Oct. 2006, doi: 10.1016/j.sigpro.2006.02.011.

[15] S. Das and S. Das, "Application of generalized fractional calculus in electrical circuit analysis and electromagnetics," in *Functional Fractional Calculus*. Berlin, Germany: Springer, 2011, pp. 387–436, doi: 10.1007/978-3-642-20545-3_8.

[16] P. E. I. Pounds, "Design, construction and control of a large quadrotor micro air vehicle," Tech. Rep., 2007.

[17] M. Ö. Efe, "Fractional order sliding mode control with reaching law approach," *Turkish J. Electr. Eng. Comput. Sci.*, vol. 18, no. 5, pp. 731–747, Jan. 2010, doi: 10.3906/elk-0906-3.

[18] N. Eluru, V. Chakour, M. Chamberlain, and L. F. Miranda-Moreno, "Modeling vehicle operating speed on urban roads in montreal: A panel mixed ordered probit fractional split model," *Accident Anal. Prevention*, vol. 59, pp. 125–134, Oct. 2013, doi: 10.1016/j.aap.2013.05.016.

[19] T. J. Freeborn, "A survey of fractional-order circuit models for biology and biomedicine," *IEEE J. Emerg. Sel. Topics Circuits Syst.*, vol. 3, no. 3, pp. 416–424, Sep. 2013, doi: 10.1109/JETCAS.2013.2265797.

[20] T. J. Freeborn, B. Maundy, and A. S. Elwakil, "Fractional-order models of supercapacitors, batteries and fuel cells: A survey," *Mater. Renew. Sustain. Energy*, vol. 4, no. 3, pp. 1–7, 2015, doi: 10.1007/s40243-015-0052-y.

[21] J. W. Gerdes, S. K. Gupta, and S. A. Wilkerson, "A review of bird-inspired flapping wing miniature air vehicle designs," *J. Mech. Robot.*, vol. 4, no. 2, May 2012, doi: 10.1115/1.4005525.

[22] G. Goh. (2017). *Additive Manufacturing in Unmanned Aerial Vehicles (UAVs): Challenges and Potential*. [Online]. Available: https://www.sciencedirect.com/science/article/pii/S127096381630503X

[23] M. Habib, W. Abdelaal, and M. Saad. (2014). *Dynamic Modeling and Control of a Quadrotor Using Linear and Nonlinear Approaches*. [Online]. Available: http://dar.aucegypt.edu/handle/10526/3965

[24] J. Han, L. Di, C. Coopmans, and Y. Chen, "Pitch loop control of a VTOL UAV using fractional order controller," *J. Intell. Robot Syst.*, vol. 73, pp. 187–195, Jan. 2014, doi: 10.1007/s10846-013-9912-9.

[25] T. Han, M. Chi, Z.-H. Guan, B. Hu, J.-W. Xiao, and Y. Huang, "Distributed three-dimensional formation containment control of multiple unmanned aerial vehicle systems," *Asian J. Control*, vol. 19, no. 3, pp. 1103–1113, May 2017, doi: 10.1002/asjc.1445.

[26] T. T. Hartley and C. F. Lorenzo, "Dynamics and control of initialized fractional-order systems," *Nonlinear Dyn.*, vol. 29, pp. 201–233, Jul. 2002, doi: 10.1023/A:1016534921583.

[27] *Improved Robust Adaptive Control of High-Order Nonlinear Systems With Guaranteed Performance—ProQuest*. Accessed: Nov. 20, 2021. [Online]. Available: https://www.proquest.com/docview/2013321917?pq-origsite=gscholar&fromopenview=true

[28] J. T. Katsikadelis and N. G. Babouskos, "Post-buckling analysis of viscoelastic plates with fractional derivative models," *Eng. Anal. Boundary Elements*, vol. 34, no. 12, pp. 1038–1048, 2010, doi: 10.1016/j.enganabound.2010.07.003.

[29] F. Kendoul, "Survey of advances in guidance, navigation, and control of unmanned rotorcraft systems," *J. Field Robot.*, vol. 29, no. 2, pp. 315–378, 2012, doi: 10.1002/ROB.20414.

[30] M. W. Khan, M. Abid, A. Q. Khan, G. Mustafa, M. Ali, and A. Khan, "Sliding mode control for a fractional-order non-linear glucose-insulin system," *IET Syst. Biol.*, vol. 14, no. 5, pp. 223–229, Oct. 2020, doi: 10.1049/iet-syb.2020.0030.

[31] J. Li and Y. Li, "Dynamic analysis and PID control for a quadrotor," in *Proc. IEEE Int. Conf. Mechatronics Autom.*, Aug. 2011, pp. 573–578, doi: 10.1109/ICMA.2011.5985724.

[32] T.-C. Lin and C.-H. Kuo, "Adaptive hybrid intelligent tracking control for uncertain fractional order chaotic systems," *Int. J. Syst. Dyn. Appl.*, vol. 1, no. 1, pp. 1–16, Jan. 2012, doi: 10.4018/ijsda.2012010101.

[33] Y. Liu and R. Bucknall, "A survey of formation control and motion planning of multiple unmanned vehicles," *Robotica*, vol. 36, no. 7, pp. 1019–1047, 2018, doi: 10.1017/S0263574718000218.

[34] R. Martin, J. J. Quintana, A. Ramos, and I. De La Nuez, "Modeling electrochemical double layer capacitor, from classical to fractional impedance," in *Proc. 14th IEEE Medit. Electrotechnical Conf.*, May 2008, pp. 61–66, doi: 10.1109/MELCON.2008.4618411.

[35] S. H. Nabavi and S. Balochian, "The stability of a class of fractional order switching system with time-delay actuator," *Int. J. Syst. Dyn. Appl.*, vol. 7, no. 1, pp. 85–96, Jan. 2018, doi: 10.4018/ijsda.2018010105.

[36] *Sliding Mode Control—An Overview | ScienceDirect Topics*. Accessed: Dec. 7, 2020. [Online]. Available: https://www.sciencedirect.com/topics/engineering/sliding-mode-control

[37] B. Wang, J. Ding, F. Wu, and D. Zhu, "Robust finite-time control of fractional-order nonlinear systems via frequency distributed model," *Nonlinear Dyn.*, vol. 85, no. 4, pp. 2133–2142, Sep. 2016, doi: 10.1007/s11071-016-2819-9.

[38] Z. Wang, X. Huang, and H. Shen, "Control of an uncertain fractional order economic system via adaptive sliding mode," *Neurocomputing*, vol. 83, pp. 83–88, Apr. 2012, doi: 10.1016/j.neucom.2011.11.018.
[39] S. L. Waslander, G. M. Hoffmann, J. S. Jang, and C. J. Tomlin, "Multi-agent quadrotor testbed control design: Integral sliding mode vs. reinforcement learning," in *Proc. IEEE/RSJ Int. Conf. Intell. Robots Syst.*, Aug. 2005, pp. 3712–3717. [Online]. Available: https://ieeexplore.ieee.org/abstract/document/1545025
[40] J. Yang, Z. Cai, Q. Lin, and Y. Wang, "Self-tuning PID control design for quadrotor UAV based on adaptive pole placement control," in *Proc. Chin. Automat. Congr.*, 2013, pp. 233–237. [Online]. Available: https://ieeexplore.ieee.org/abstract/document/6775734/
[41] Q. Yang, D. Chen, T. Zhao, and Y. Chen, "Fractional calculus in image processing: A review," 2016, *arXiv:1608.03240*.
[42] B. Zhu, K. Guo, and L. Xie, "A new distributed model predictive control for unconstrained double-integrator multiagent systems," *IEEE Trans. Autom. Control*, vol. 63, no. 12, pp. 4367–4374, Dec. 2018. [Online]. Available: https://ieeexplore.ieee.org/abstract/document/8325302/
[43] Y. Luo, L. Di, J. Han, and H. Chao. (2010). *VTOL UAV Altitude Flight Control Using Fractional Order Controllers*. [Online]. Available: https://digitalcommons.usu.edu/aggieair_pres/15/
[44] A.-W.-A. Saif, A. Aliyu, M. A. Dhaifallah, and M. Elshafei, "Decentralized backstepping control of a quadrotor with tilted-rotor under wind gusts," *Int. J. Control, Autom. Syst.*, vol. 16, no. 5, pp. 2458–2472, Oct. 2018.
[45] A. W. A. Saif, M. Ataur-Rahman, S. Elferik, M. F. Mysorewala, M. Al-Dhaifallah, and F. Yacef, "Multi-model fuzzy formation control of UAV quadrotor," *Intell. Automat. Soft Comput.*, vol. 27, no. 3, pp. 817–834, 2021.
[46] A. W. Saif, N. Alabsari, S. E. Ferik, and M. Elshafei, "Formation control of quadrotors via potential field and geometric techniques," *Int. J. Adv. Appl. Sci.*, vol. 7, no. 6, pp. 82–96, Jun. 2020.
[47] A. Kilbas, H. M. Srivastava, and J. J. Trujillo, *Theory and Applications of Fractional Differential Equations*. 2006.

ABDUL-WAHID A. SAIF received the B.Sc. degree from the Physics Department, King Fahd University of Petroleum & Minerals (KFUPM), Dhahran, Saudi Arabia, the M.Sc. degree from the Systems Engineering Department, KFUPM, and the Ph.D. degree from the Control and Instrumentation Group, Department of Engineering, Leicester University, Leicester, U.K. He was a Research Assistant with the SE Department and a Lecturer with the Electrical Engineering Department and the Physics Department, KFUPM, where he is currently a Professor in control and instrumentation with the Control and Instrumentation Engineering Department (CIE). After finishing the Ph.D. degree, he joined in systems engineering. He taught several courses in modeling and simulation, digital control, digital systems, microprocessor and microcontrollers in automation, optimization, numerical methods, PLCs, process control, and control system design. He has supervised/co-supervised many Ph.D. and M.Sc. students. He has published more than 115 papers/patents in reputable journals and conferences. His research interests include simultaneous and strong stabilization, robust control and $H\infty-$optimization, instrumentation, computer control, the control of time-delay systems, and wire and wireless network control.

KHALED BIN GAUFAN received the B.S. and M.S. degrees in control and instrumentation system engineering from the King Fahd University of Petroleum & Minerals, Dhahran, Saudi Arabia, in 2018 and 2021, respectively, where he is currently pursuing the Ph.D. degree with the Department of Control and Instrumentation Engineering.

SAMI EL-FERIK received the B.Sc. degree in electrical engineering from Laval University, Quebec City, Canada, and the M.S. and Ph.D. degrees in electrical and computer engineering from Ecole Polytechnique, University of Montreal, Montreal, Canada. He is currently a Professor in control and instrumentation with the Department of System Engineering, King Fahd University of Petroleum & Minerals. His Ph.D. work on flexible manufacturing systems modeling and control, was co-supervised in mechanical engineering. After completion of the Ph.D. and postdoctoral research positions, he was with the Research and Development Center of Systems, Controls, and Accessories, Pratt and Whitney, Canada, as a Staff Control Analyst. His research interests include sensing, monitoring, control with strong multidisciplinary research and applications, the control of drug administration, process control and control loop performance monitoring, the control of systems with delays, modeling and control of stochastic systems, the analysis of network stability, condition monitoring, and condition-based maintenance.

MUJAHED AL-DHAIFALLAH received the B.A. and M.S. degrees in systems engineering from the King Fahd University of Petroleum & Minerals (KFUPM), Dhahran, Saudi Arabia, and the Ph.D. degree in electrical and computer engineering from the University of Calgary, Calgary, AB, Canada. Since 2009, he has been an Assistant Professor in systems engineering with KFUPM, where he is currently the Chairman. His work has been published in numerous scholarly and industry journals and at conferences, including IEEE Transactions on Control Systems Technology, the 22nd European Symposium on Computer Aided Process Engineering, the 18th IFAC World Congress, and the Eighth International Multi-Conference on Systems, Signals & Devices. His current research interests include developing systems identification techniques for applications ranging from neuromuscular control and robotics to power systems and electrical machines.